S. Yoon

Self-assembly of Helical structure by defected nanosheet

Sang-hee Yoon, and Eunji Sim*

Department of Chemistry, Yonsei University, 50, Yonsei-ro, Seodaemun-gu, Seoul, 120-749, Korea.
Received Date; Accepted Date (to be inserted by the publisher after your manuscript is accepted)

Abstract: A helical nanosturctrue can be obtained by self-assembly method. Utilizing DPD simulation coarse-grained model, we patterned 2D layer nanosheets with repeated diagonal defects and grafts, and programed to self-roll into hollow helix structure. The defected pattern side caused anisotropy, and formed helix or helix-like structure. This opens the possibility to control the helix pitch or cavity radius. In this work, we designed several patterns about diagonal defect with a variety of defect side densities and defect widths and then simulation was carried out. Thus, our results have that parameters are affecting self-assembly of nanosheets and their conformation.

Keywords: Self-assembly, DPD, helix structure, coarse-grained model

Introduction

Helix nanotubes are receiving considerable attention as potential high-tech materials due to their different functions, depending on the nature of the structural characteristics and components. And helix structures are omnipresent materials in biological self-assembled structures[1,6] also in medical and industrial hollow cavity enables potential applications in nanotechnology encapsulation. As a result self-assembly of helix structure is a simple and economic method to constructing the organized molecules[1,7] for diverse fields[6]. The interest in the self-assembly of helix structure has propelled both theoretic and experimental studies. The size of interior cavity is one of the most important features of nanotubes as a deliver material.

Although varius fabrication methods of helical polymer have been made their exact pitch and helical sense remains unsolved.[2,5,6]. In our previous report[4] we suggested a defected nanosheets to control the size of nanotube internal cavity. The 2D layer attached with amphiphile coils application was also used in this simulation.

Theory and Computational Method

Nnanosheets are described by DPD coarse-grained model which was presented at Figure 1. Nanolayer is rectangular shape(40×150) and every *i*th and *j*th beads, which there distance is r_{ij}, are connected with harmonic spring, $F_{ij} = -k_{layer}(r_{ij} - \bar{r})^2$. k_{layer} is force constant, r_{ij} is distance between *i*th and *j*th beads, and $\bar{r}$ is equilibrium distance. Layer beads are of all the same kind and also their horizontal and vertical force constants are equal. Each side of layer, tether coil consiste of five particles, are attached at hexagonal point to prevent overcrowding as depicted at Figure 1(a). At reference side all hexagonal points are attached with graft coil and in this case, reference side density would be $\rho_R = 1.0$. While at defect side basically graft coils are attached at hexagonal point but in defect side they have pattern with regular interval defect. Defect width ranges from 3 to 10 in integer number, and defect line angle is 30 degree from a vertical axis(figure 2.). Defect side density ρ_D is the ratio about reference density ρ_R, so that it has more defect line and larger defect width then ρ_D as gets lower value. In this simulation four kinds of density($\rho_D = 0.4, 0.5, 0.6, 1.0$) were used to compute.

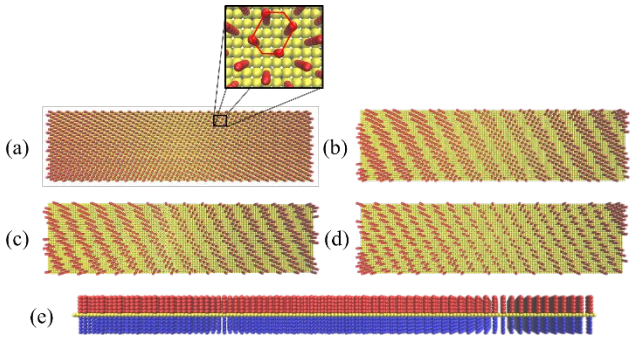

Figure 1. Various kind of nanosheet samples. Graft coils are attached at layer hexagonal point and making hexagonal packing. no-defect nanosheet (a), and gG-dD examples (b), (c), (d). Each (b), (c), (d) figure graft and density width are 7,8G-5D, 5G-5D and 3,4G-5D and

each defect side density $\boldsymbol{\rho_D}$ are 0.6, 0.5, 0.4. It designed symmetrical.

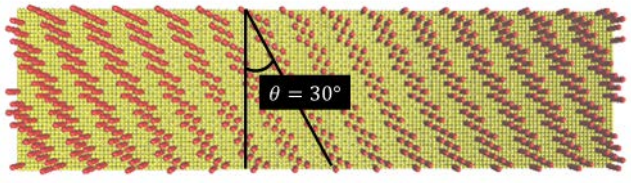

Figure 2. Angle between vertical axis and defect diagonal line is always 30 degree.

To detect the influence of defect to sheet transformation we use DPD(Dissipative Particle Dynamics) method. DPD is one of molecular dynamics, and it uses classical mechanics to run simulation. *i*th total force(F_i) is the sum of conservative force(F_{ij}^C), dissipative force(F_{ij}^D) and random force(F_{ij}^R) between *i*th and *j*th beads.

$$F_i = \sum_{i \neq j} \left(F_{ij}^C + F_{ij}^D + F_{ij}^R \right)$$

$$F_{ij}^C = a_{ij}\left(1 - \frac{r_{ij}}{r_c}\right)\hat{r}_{ij}$$

$$F_{ij}^D = -\gamma\left(1 - \frac{r_{ij}}{r_c}\right)^2 (\hat{r}_{ij} \cdot \vec{v}_{ij})\hat{r}_{ij}$$

$$F_{ij}^R = \sigma\left(1 - \frac{r_{ij}}{r_c}\right)\zeta_{ij}(\Delta t)^{-1/2}\hat{r}_{ij}$$

r_{ij} is $r_{ij} = |r_{ij}\hat{r}_{ij}| = |r_i - r_j| \leq r_c$, and if r_{ij} larger than r_c, the cutoff distance, then each force will be zero. The cutoff distance is $r_c = 1.0$ at this calculation. a_{ij} is repulsion strength works between *i*th and *j*th particle, dissipative strength $\gamma = 4.5$. Random noise strength is $\sigma = 3.0$ to control the system temperature as $\sigma^2 = 2\gamma k_B T$. Δt is a propagation time step and ζ_{ij} is a Gaussian random number with zero mean and unit variance. [3]

Graft coil						Nanolayer(N)		
$a_{\alpha\alpha}$ $(\alpha = R, D, S)$	a_{RD}	a_{RS}	a_{DS}	k_{coil}	$\bar{r}_{coil}$	$a_{N\alpha}$ $(\alpha = R, D, S)$	k_{sheet}	$\bar{r}_{sheet}$
25	25	25	25	25	0.5	30	50	0.5

Table 1. DPD potential parameters: repulsion parameters($\boldsymbol{a_{\alpha\beta}}$), bonding force constant(**k**) and equilibrium bond distance($\bar{r}$). Subscript R, D, S, N represent reference side graft coil, defect side graft coil, solvent, and nanolayer.

The DPD potential parameters in Table 1. was used for this model. Repulsive parameters $a_{\alpha\alpha}$ was equal to 25, and $a_{N\alpha}$ was equal to 30. Force constants were also equal to 25 except sheet layer, and all bond distances have the same value.

Most simulation was carried out with LAMMPS package with a time step $\Delta t = 0.04\tau$ and the temperature was maintained at 0.3 in DPD reduced units. For all simulation the periodic boundary condition was applied for all directions and nanosheets were performed at simulation box($40 \times 80 \times 40$). Simulation box was filled with theta solvent. The total number of beads are 384,000.

Results and Discussion

Before making defected nanosheets, we made no-defected sheet, which was shown in figure 1(a); the reference nanosheet and its density is $\rho_R = \rho_D = 1$. This polymer waves and never rolls or makes cavity. Lyophilic tether coils spread into solvent and prevent lyophobic layer from getting aggregate but it always make fluctuating motion. This movement is shown in figure 3.

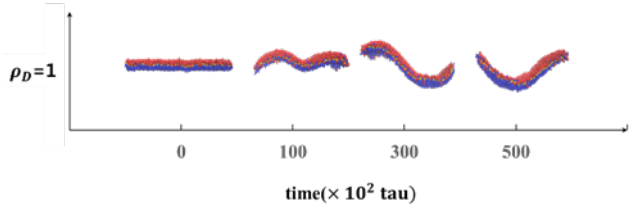

Figure 3. Initial structure of no-defect nanosheet and conformation change by time evolution. System runs until 50,000τ. Nanosheet makes sinuous movements in time.

On the other hand, diagonal defected nanosheets make a helix or helix-like structure. End of the sheets start to roll up in solvent filled circumstance and getting to meet their side edge of sheet. Scroll direction was determined by defect angle that is presented in figure 2. All defected-sheets have diagonal angle and angle value is 30 degree.

To analyze sheet form we used radius of gyration equation. The radius of gyration, $\tilde{R}_g(t)$, has three components of gyration tensor, and their equation was expressed as in the following.

$$\tilde{R}_g(t) = \sqrt{\bar{R}_{xx}{}^2(t) + \bar{R}_{yy}{}^2(t) + \bar{R}_{zz}{}^2(t)}$$

The elements are defined as

$$R_{\gamma\delta} = \frac{1}{M_{layer}} \sum_{i=1}^{M_{layer}} (\gamma_i - \gamma_{CM})(\delta_i - \delta_{CM})$$

where γ_i and δ_i are the x, y, z coordinates of the ith bead of the layer. γ_{CM} and δ_{CM} are center of mass of the layer consisting of M_{layer} beads. In figure. 4, black line shows $\tilde{R}_g(t)$ and colored line presents the three components, $\bar{R}_{\alpha\alpha}(t)$. Red line shows the longest principle moments of gyration which denotes vertical axis of rolled nanosheet polymer. Gray line presents horizontal axis of principle moment, and blue line presents another horizontal axis which denotes thickness of polymer.

The simulation results about figure 1. (b), (c), (d) ROG change and morphology transformation shows in figure 4. Early phase of ROG graph, ROG changes drastically and gradually converge to regular value. To designate the stabilization phase, we use standard deviation. When standard deviation value gets lower than 0.2. we provisionally define that moment as end of simulation. When defect side density gets bigger then ROG value get lower. This means the length of structure which lies on major principle axis gets shorter. Not only radius of gyration, we also use pitch and radius to analyze sheet conformation.

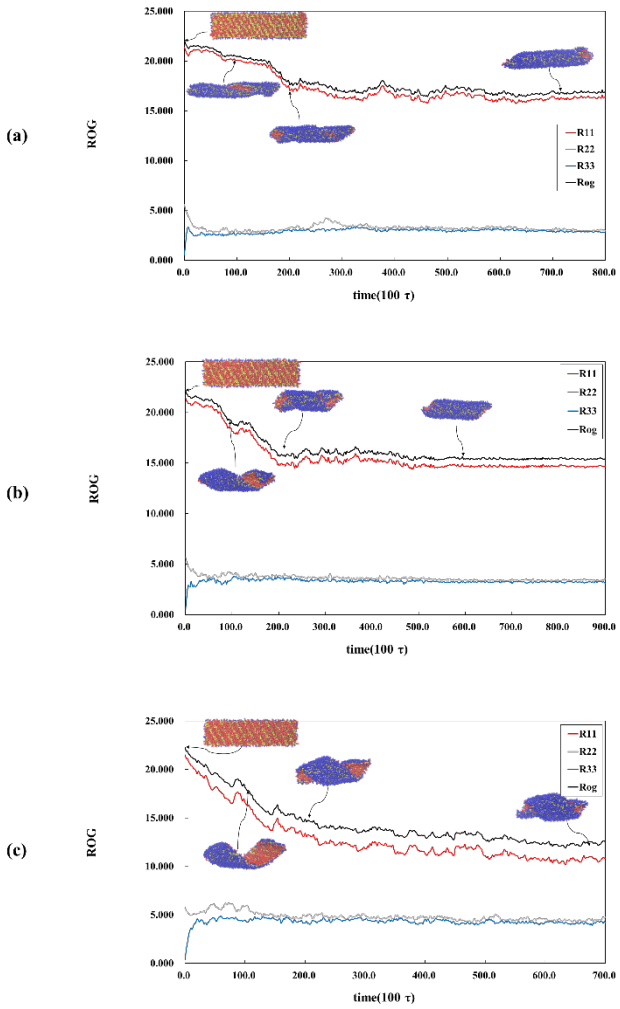

Figure 4. After initialization of nanosheet's and ROG, conformation change by time evolution. Initial structure of (a), (b), (c) presents in figure (b), (c), (d). and their graft-defect width are 3,4G-5D, 5G-5D and 7,8G-5D.

Varity of density and defect width are 0.4, 0.5, 0.6 and 3D to 10D. Almost all nanosheets made helix or helix-like conformation. Figure 5. presents ROG, pitch and radius values according to defect width. In figure 5. ROG and pitch value get lower when defect side density value and defect width get bigger, while radius value get larger. It means defect side density and defect width affect to ROG, pitch and radius. As shown in figure 5(b), 3D defect width in $\rho_D = 0.4$, graft coils are few and defect width are small its defect side might affected as random graft coiled nanosheet not as diagonal designed nanosheet. As a result, 2G-3D($\rho_D = 0.4$) formed cylindrical nanotube so pitch value doesn't exist and gets largest ROG value. When defect width gets bigger ROG get lower and this tendency also shown in $\rho_D = 0.5$. But when it gets in $\rho_D = 0.6$, ROG looks converse. This tendency alike in pitch.

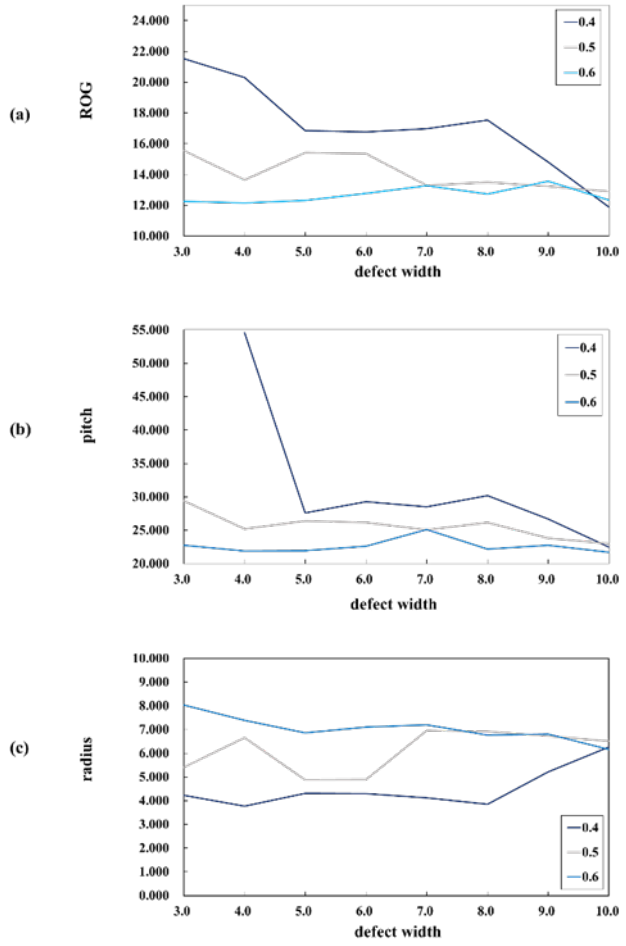

Figure 5. ROG, pitch and radius values according to defect width.

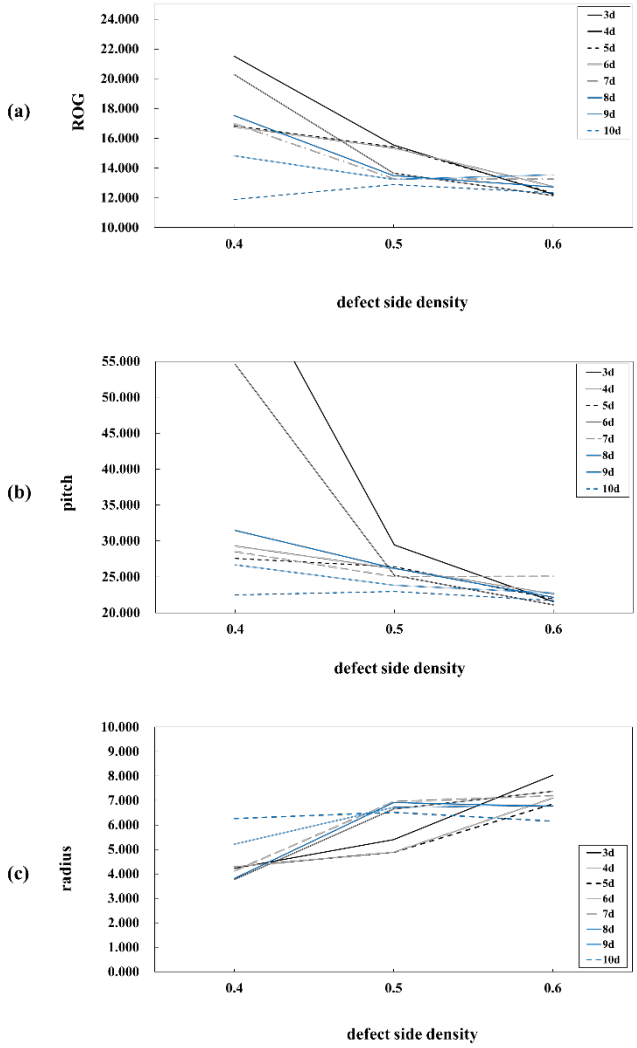

Figure 6. ROG, pitch and radius value according to defect side density.

Figure 6. presents ROG, pitch, radius value according to defect side density(ρ_D). Different from figure 5. it is hard to read the meaning of each values. When these nanosheets were visualized in VMD program, there were only few complete helix structure existing. Most of polymers layer didn't match edge by edge, as a result their conformation didn't fixed. Only 5D at defect side density 0.5 and 5D, 6D, 7D, 8D at defect side density 0.4 form complete helix structure. When we observed other nanosheets with VMD, end of sheet layer start to roll and if end of sheet layer rolled excessively, than nanosheets make helix-like structure. Once end of sheet layer form over-rolled conformation there are not only layer-layer attraction but also tether coil-tether coil attraction. Thus it is assumed that it would be hard to spread again. Most of nanosheets form like figure 6(b). and then make a fluctuant movement at that state.

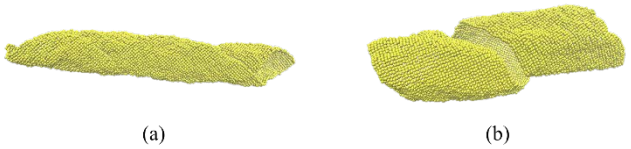

(a) (b)

Figure 7. Extract only layer of 6D defected nanosheets. Each (a), (b) defect side density is 0.4 and 0.6. (a) form complete helix structure and (b) form helix-like structure.

Conclusion

Using DPD simulation of coarse-grained diagonal defected nanosheet model, we observe their self-assembly with defect designed nanosheet. At previous experiments we found controlling the internal cavity by parallel to vertical and horizontal line defect was possible[4], and applied that method to diagonal defect. As a result sheets rolled very well but not like complete helix structure. Sometimes we could find well-assembled helix structure. If we happen to find the specific condition of making complete helix, it's internal cavity and polymer length could be controlled to make specific conformation.

Acknowledgments. This work has been supported by the project EDISON (EDucation-research Integration through Simulation On the Net), Chemistry.

References

1. Barclay, T. G., Constantopoulos, K., & Matisons, J. *Chemical Reviews*, **2014**, 114(20), 10217–10291.
2. E. Yashima, *Polymer Journal*, **2010**, Vol.42, p.3-16
3. Pivkin, I. V, Caswell, B., & Karniadakis, G. E. *Reviews in Computationa Chemistry*, 2011, Vol. 27, 27, 85–110.
4. Han, M., Hyun, J., & Sim, E. *Soft Matter*, 2015, 11(18), 3714–3723.
5. Zastavker, Y. V, Asherie, N., Lomakin, a, Pande, J., Donovan, J. M., Schnur, J. M., & Benedek, G. B. *Proceedings of the National Academy of Sciences of the United States of America*, **1999**, 96(14), 7883–7887.
6. Duan, Y., Yan, S., Zhou, X., Xu, W., Xu, H., Liu, Z., Yao, L. *Chemical Communications* (Cambridge, England), **2014**, 50, 8335–8.
7. Mann, S. *Nature Materials*, **2009**, 8(10), 781–792.